KSTLE International Journal, Vol. 7, No. 2, December 2006, pp. 27-34

A Study on the Air Foil Journal Bearing Analysis with Perturbed Rarefaction Coefficients

Yong-Bok Lee†, Dong-Jin Park, Chang-Ho Kim and Gun-Hee Jang*

Tribology Research Center, Korea Institute of Science and Technology, Seoul, Korea
**Department of Mechanical Engineering, Hanyang University, Seoul, Korea*

Abstract: Knudsen number is the ratio of molecular mean free path versus film thickness and the criterion to determine the flow form. When its value is lower than 0.01, the flow can be assumed to has no slip boundary condition. And in the case that the value is between 0.01 and 10, then the flow has slip boundary condition at both the adjacent walls. The condition of the air flow between the rotating journal and top foil in the air foil bearing is determined by the rotating speed and load, and the Knudsen number is also varied by those values. Because the molecular mean free path is variable to the pressure and temperature, more exact formulation is necessary to understand and analyze the flow regime. In this study, the analysis considering Knudsen number formulated with those variables (pressure, temperature and film thickness) was executed. The approximate value was examined using the equation to confirm whether the flow has the slip or no-slip boundary condition. From the analytic investigation, it was decided to range approximately 0.01 to 1.0 and the flow can be supposed to have the slip boundary condition. Under the condition of the slip flow, the static characteristics of the air foil bearing were examined using modified Reynolds equations. The results were compared with those considering no slip condition. It shows that the slip condition makes the flow decelerates and the load carrying capacity decreases compared with no slip condition. And as the bearing number and eccentricity ratio increase, the load carrying capacity also increased at both the cases. From this result, it can be supposed that the bearing torque also increases. In the analysis of the dynamic characteristics, the perturbed Knudsen number was taken into consideration. Because the Knudsen number is expressed as the terms of each variable, the perturbed equation can be simply derived. The results of both cases considering and not considering Knudsen number were compared each other. In the case of the direct terms of the stiffness and damping coefficients, the difference between both cases was little and increased as the bearing number and eccentricity ratio increased. And the cross terms have less or more differences.

Keywords: Air foil bearing, knudsen number, perturbation method, slip flow

1. Introduction

From the need for the bearing systems which are able to overcome the limitations of the existing liquid lubricated bearing and rolling element bearings, the foil bearing has been widely studied. Since first devised, the structure shape of the foil bearing has been changed to increase the load carrying capacity and damping capacity. The first foil bearing, tension tapered foil bearing, simply consists of smooth foil sheets of which the both ends are fixed. And this type foil bearing in which the dominant mode of elastic deformation is extension has load carrying capacity using the tension of the foil [1]. The multiple leaf foil bearing, the second type foil bearing has the structure that several foil sheets are fold on each other. And the bending rigidity of the foil plays a role to the bearing compliance [2]. Because both the bearing had some disadvantages same as low load carrying and damping capacities, however, they aren't suitable as the bearing element for the high speed turbo machinery and the bump type foil bearing were devised as the next generation foil bearing [3-4]. The air foil bearing simply consists of bump and top foil. The bump foil has the stiffness and flexibility and this characteristics make it has high load carrying capacity and more stability under sudden disturbance. And it has several advantages as same as the high temperature endurance, no limit DN value and etc. With these merits, many studies to use as the bearing part of the commercial rotating machinery as same as the gas turbine, turbocharger, high speed motor, air blower and etc. have been conducted. Recent works to develop the self acting coating material for high temperature region help the air foil bearing to approach commercialization more closely [5-6]. The air foil bearing has the initial clearance of 40~60 mm and the general flow between the top foil and rotating journal can be assumed to the slip flow determined by the Knudsen number criterion. Though the flow regime is slip flow, previous works didn't consider the effect and Knudsen number were introduced as constant about the temperature [7]. Thus, to calculate the dynamic characteristics of the air foil bearing with the perturbed rarefaction coefficient was attended with difficulties. In this study, the air foil journal bearing analysis considering the slip flow were conducted with the Knudsen number equation for the purpose of simplification in

†Corresponding author; lyb@kist.re.kr
Tel: +82-2-958-5663, Fax: +82-2-958-5659

Nomenclature

c	: Bearing initial clearance [m]
c_e	: Bump damping coefficient [N · sec/m]
d_{gas}	: Diameter of gas molecule [m]
e	: Eccentricity [m]
h	: Thin film height [m]
k_e	: Bump stiffness [N/m]
N_A	: Avogadro's number
p	: Pressure [N/m^2]
p_a	: Ambient pressure [N/m^2]
R	: Gas constant
T	: Temperature
u	: Angular velocity of the air flow [m/s]
u_r	: Linear velocity of the journal [m/s]
v	: Axial velocity of the air flow [m/s]
w	: Bump deflection [m]
x,y,z	: Rectangular coordinates
Kn	: Knudsen number
α	: Bump compliance
ε	: Eccentricity ratio [m]
ρ	: Density of the gas [kg/m^3]
λ	: Molecular mean free path [m]
μ	: Viscosity of the gas
ϕ_0	: Attitude angle [degree]
Λ	: Bearing number, Compressibility
γ	: Whirl frequency ratio
φ^p	: Rarefaction gas constant

analysis procedure and the results were compared with those considering no slip condition to confirm the slip flow effect. To calculate the pressure distribution of the thin air film between the rotating journal and top foil, Navier-stokes equation with slip boundary condition and continuity equation were modified into Reynolds equation with rarefaction gas coefficient. The rarefaction gas coefficient is the function of film thickness and molecular mean free path, and molecular mean free path can be expressed as the function about pressure and temperature. And the equation was modified using the equation about the coefficient. Modified Reynolds equation was discretized using central difference method. And the pressure distribution was obtained by successive under relaxation method. Perturbation method, the reaction due to small displacement of the rotor at equilibrium state, was used to calculate the dynamic characteristics, stiffness and damping, considering the perturbed rarefaction coefficients.

2. Basic theory and bearing model

2.1. Thin air film analysis

Figure 1 shows the air foil bearing configuration which the bump and top foil are inserted between the bearing housing and rotating journal. The flow of the thin film between the top foil and rotating journal can be assumed to the laminar flow between two short flat surfaces. And it can be calculated using

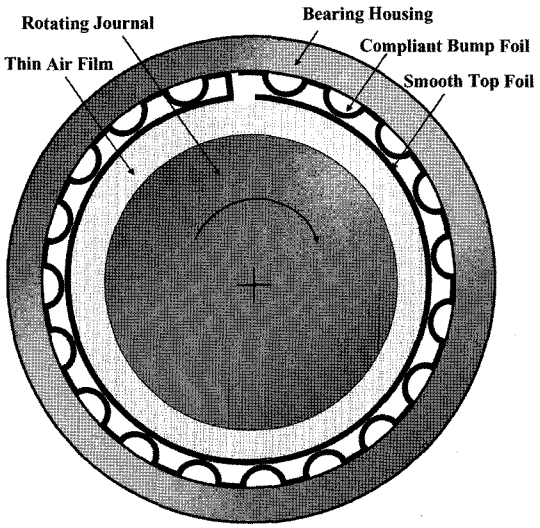

Fig. 1. Air foil bearing configuration with the bump and smooth top foil sheets.

continuity equation and x, y, and z directions Navier-Stokes equations as following equations:

$$\frac{\partial}{\partial x}[\rho\int_0^h u dz] + \frac{\partial}{\partial y}[\rho\int_0^h v dz] + \frac{\partial}{\partial t}(\rho h) = 0 \tag{1}$$

$$\frac{\partial p}{\partial x} = \mu\frac{\partial^2 u}{\partial z^2}, \quad \frac{\partial p}{\partial y} = \mu\frac{\partial^2 v}{\partial z^2}, \quad \frac{\partial p}{\partial z} = 0 \tag{2}$$

Here, r is the density of air, m is the viscosity, and u and v represent the velocity to the directions of x and y, respectively. Because the working fluid is the compressible gas, the density in the bracket can't be eliminated. And multiplying gas constant, R, and temperature, T, to each terms, the density can be derived into pressure, p. The x direction velocity of the flow can be calculated integrating Navier-Stokes equation twice. It is as follows:

$$u = \frac{1}{2\mu}\frac{\partial p}{\partial x}z^2 + C_1 z + C_2 \tag{3}$$

Here, C_1 and C_2 represent the integral constants. To obtain those constants, the velocity at the wall is necessary and it can be expressed using 1st order slip boundary condition.

$$u(z=0) = u_r + \lambda\left.\frac{\partial u}{\partial z}\right|_{z=0}, \quad u(z=h) = -\lambda\left.\frac{\partial u}{\partial z}\right|_{z=h} \tag{4}$$

Where, u_r is the linear velocity of the rotating journal, h is the air film thickness and γ is molecular mean free path. Using above boundary condition, the velocity profile to the x-direction can be derived as follows:

$$u = -\frac{1}{2\mu}\frac{\partial p}{\partial x}(h\lambda + hz - z^2) + u_r\left(1 - \frac{z+\lambda}{z+2\lambda}\right) \tag{5}$$

Similarly, the velocity profile to the y-direction, side flows, can be derived as follows:

$$v = -\frac{1}{2\mu}\frac{\partial p}{\partial y}(h\lambda + hz - z^2) \tag{6}$$

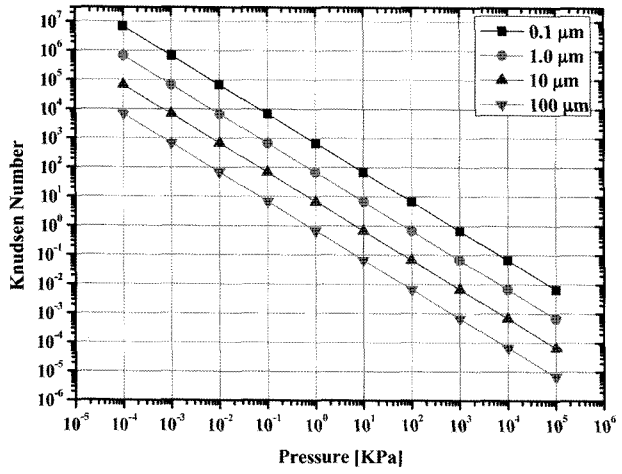

Fig. 2. Knudsen number at the various conditions of the film thickness versus environmental pressure.

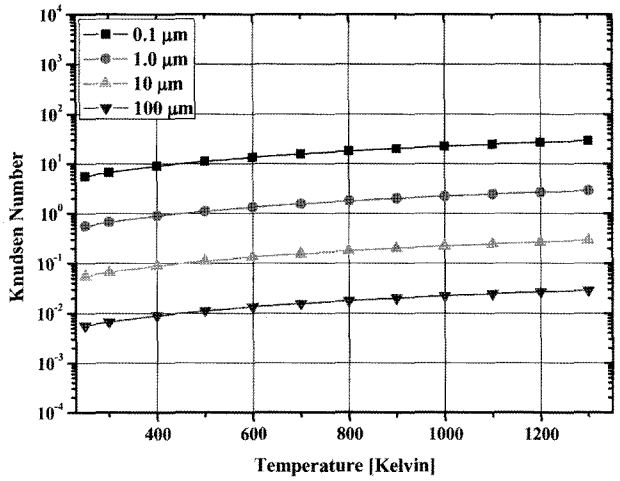

Fig. 3. Knudsen number at the various conditions of the film thickness versus environmental temperature.

Introducing the above equations to the continuity equation, the modified Reynolds equation can be expressed as following vector form:

$$\nabla \cdot \left(-\frac{1}{12\mu} \varphi^P p h^3 \nabla p + \frac{\bar{U}}{2} p h \right) + \frac{\partial}{\partial t}(ph) = 0 \tag{7}$$

Here, $\bar{U}$ is the linear velocity vector. φ^P is the rarefaction gas coefficient and determined by film thickness and molecular mean free path as follows:

$$\varphi^P = 1 + 6\frac{\lambda}{h} = 1 + 6\mathrm{Kn} \tag{8}$$

Here, Kn represent the Knudsen number. Knudsen number is the criterion to determine the flow regime. It can be expressed as following analytic form [8].

$$\mathrm{Kn} = \frac{RT}{\pi\sqrt{2} d_{gas}^{\,2} N_A P h} = \frac{0.067}{Ph} \tag{9}$$

Where, R, T, d_{gas} and N_A represent the gas constant, temperature, diameter of the gas molecule and Avogadro's number (~6.02×10^{23}), respectively.

Figure 2 and 3 show the Knudsen number variation versus the temperature and pressure. As the pressure increases, Knudsen number decreases at constant film thickness due to decreased molecular mean free path by the constraints of the air molecular. Otherwise, as the temperature increases, it also increases. It is because the motion of the molecular becomes more actively.

$$p - p_a = k_e w + c_e \frac{dw}{dt} \tag{10}$$

Here, P_a, K_e, C_e and w represent ambient pressure, stiffness of the elastic foundation, damping and deflection, respectively. The air film thickness is determined by initial clearance, c, eccentricity, e, and bump deflection. And it can be expressed as following equation.

$$h = c - e\cos(\theta - \phi_0) + w \tag{11}$$

Where, f represent the attitude angle. The bump deflection is dependent on the pressure, the bump compliance, and varied with the bump foil configuration. In this study, the results under several compliances were analyzed and investigated.

2.2. Elastic foundation model and analysis

The corrugated bump foil is the important element to generate Coulomb damping of the structure parts. And under sudden disturbance, its flexibility makes the journal rotates safely. In this study, several assumptions were taken into consideration to analyze the bump foil.

1. The stiffness and damping of the bump foil is constant and uniform over bearing surface.
2. The bump foil deflection generates at the position where the load acts. And the interaction among bumps can be ignored.

Using above two assumptions, the bump foil modelcan be expressed as following equations:

2.3. Boundary conditions

Generally, both sides, the start and end boundaries, of the bearing are assumed to the ambient pressure. It can be expressed as following analytic form.

$$p(z = 0, L) = p_a \tag{12}$$

$$p(\theta = \theta_1, \theta_1 + 2\pi) = p_a \tag{13}$$

Here, L is the bearing axial length and q_1 is the start angle of the elastic foundation.

2.4. Numercal regimes

The perturbation method was used to calculate the characteristics of the air foil bearing. Introducing the perturbed pressure, film height, bump deflection and rarefaction gas coefficients due to small displacement at the static equilibrium

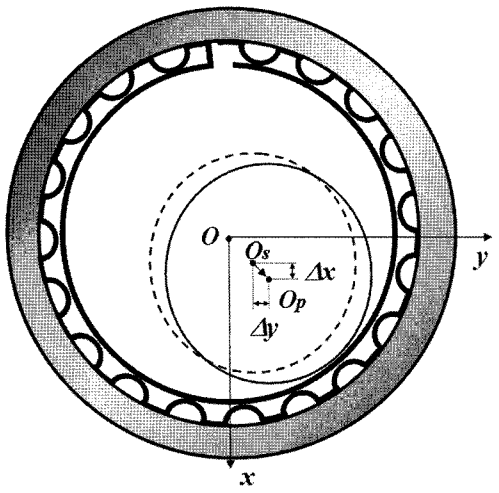

Fig. 4. The perturbation method for the static journal equilibrium position.

position to the modified Reynolds equation, a zeroth order equation and four 1st order equations can be obtained. Figure 4 shows the perturbed rotor configuration. Following equations represent the variables expressed using the values at the equilibrium state and perturbed.

$$p = p_0 + p_x\Delta x + p_y\Delta y + p_{\dot{x}}\Delta\dot{x} + p_{\dot{y}}\Delta\dot{y} \tag{14}$$

$$h = h_0 + h_x\Delta x + h_y\Delta y + h_{\dot{x}}\Delta\dot{x} + h_{\dot{y}}\Delta\dot{y} \tag{15}$$

$$w = w_0 + w_x\Delta x + w_y\Delta y + w_{\dot{x}}\Delta\dot{x} + w_{\dot{y}}\Delta\dot{y} \tag{16}$$

$$\varphi^P = \varphi_0^P + \left(\frac{\partial\varphi^P}{\partial p}\right)_0\Delta p + \left(\frac{\partial\varphi^P}{\partial h}\right)_0\Delta h \tag{17}$$

Here, subscript *0* present the equilibrium state and *x*, $\dot{x}$, *y*, and $\dot{y}$ present each direction perturbation amplitude and velocity. The perturbed rarefaction coefficient can be expressed as following equation using equation (9).

$$\varphi^P = \varphi_0^P + \frac{0.402}{p^2h}\Delta p + \frac{0.402}{ph^2}\Delta h \tag{18}$$

When the perturbed journal vibrate with constant frequency, the relationship between the perturbed motion and the perturbed acceleration can be expressed as follows:

$$\Delta\ddot{x} = -\upsilon^2\Delta x, \quad \Delta\ddot{y} = -\upsilon^2\Delta y \tag{19}$$

Using the non-dimensional variables, the perturbed equations can be derived as following forms:

$$\bar{\nabla}\cdot(-\varphi_0^p\bar{p}_0\bar{h}_o^3\bar{\nabla}\bar{p}_o + \vec{\Lambda}\bar{p}_o\bar{h}_o) = 0 \tag{20}$$

$$\bar{\nabla}\cdot(-\varphi_0^p\bar{p}_0\bar{h}_o^3\bar{\nabla}\bar{p}_x - \varphi_0^p\bar{p}_x\bar{h}_o^3\bar{\nabla}\bar{p}_o - 3\varphi_0^p\bar{p}_0\bar{h}_o^2\bar{h}_x\bar{\nabla}\bar{p}_o) +$$
$$\bar{\nabla}\cdot(-(\partial\varphi^P/\partial p)_0\bar{p}_x\bar{p}_0\bar{h}_o^3\bar{\nabla}\bar{p}_o - (\partial\varphi^P/\partial h)_0\bar{p}_0\bar{h}_o^2\bar{h}_x\bar{\nabla}\bar{p}_o) +$$
$$\bar{\nabla}\cdot\vec{\Lambda}(\bar{p}_x\bar{h}_o + \bar{p}_o\bar{h}_x) - 2\Lambda\gamma(\bar{p}_x\bar{h}_o + \bar{p}_o\bar{h}_x) = 0 \tag{21}$$

$$\bar{\nabla}\cdot(-\varphi_0^p\bar{p}_0\bar{h}_o^3\bar{\nabla}\bar{p}_{\dot{x}} - \varphi_0^p\bar{p}_{\dot{x}}\bar{h}_o^3\bar{\nabla}\bar{p}_o - 3\varphi_0^p\bar{p}_0\bar{h}_o^2\bar{h}_{\dot{x}}\bar{\nabla}\bar{p}_o) +$$
$$\bar{\nabla}\cdot(-(\partial\varphi^P/\partial p)_0\bar{p}_{\dot{x}}\bar{p}_0\bar{h}_o^3\bar{\nabla}\bar{p}_o - (\partial\varphi^P/\partial h)_0\bar{p}_0\bar{h}_o^3\bar{h}_{\dot{x}}\bar{\nabla}\bar{p}_o) +$$
$$\bar{\nabla}\cdot\vec{\Lambda}(\bar{p}_{\dot{x}}\bar{h}_o + \bar{p}_o\bar{h}_{\dot{x}}) - 2\Lambda\gamma(\bar{p}_{\dot{x}}\bar{h}_o + \bar{p}_o\bar{h}_{\dot{x}}) = 0 \tag{22}$$

$$\bar{\nabla}\cdot(-\varphi_0^p\bar{p}_0\bar{h}_o^3\bar{\nabla}\bar{p}_y - \varphi_0^p\bar{p}_y\bar{h}_o^3\bar{\nabla}\bar{p}_0 - 3\varphi_0^p\bar{p}_0\bar{h}_o^2\bar{h}_y\bar{\nabla}\bar{p}_o) +$$
$$\bar{\nabla}\cdot(-(\partial\varphi^P/\partial p)_0\bar{p}_y\bar{p}_0\bar{h}_o^3\bar{\nabla}\bar{p}_0 - (\partial\varphi^P/\partial h)_0\bar{p}_0\bar{h}_o^3\bar{h}_y\bar{\nabla}\bar{p}_0) +$$
$$\bar{\nabla}\cdot\vec{\Lambda}(\bar{p}_y\bar{h}_o + \bar{p}_o\bar{h}_y) - 2\Lambda\gamma(\bar{p}_y\bar{h}_o + \bar{p}_o\bar{h}_y) = 0 \tag{23}$$

$$\bar{\nabla}\cdot(-\varphi_0^p\bar{p}_0\bar{h}_o^3\bar{\nabla}\bar{p}_{\dot{y}} - \varphi_0^p\bar{p}_{\dot{y}}\bar{h}_o^3\bar{\nabla}\bar{p}_0 - 3\varphi_0^p\bar{p}_0\bar{h}_o^2\bar{h}_{\dot{y}}\bar{\nabla}\bar{p}_0) +$$
$$\bar{\nabla}\cdot(-(\partial\varphi^P/\partial p)_0\bar{p}_{\dot{y}}\bar{p}_0\bar{h}_o^3\bar{\nabla}\bar{p}_0 - (\partial\varphi^P/\partial h)_0\bar{p}_0\bar{h}_o^3\bar{h}_{\dot{y}}\bar{\nabla}\bar{p}_0) +$$
$$\bar{\nabla}\cdot\vec{\Lambda}(\bar{p}_{\dot{y}}\bar{h}_o + \bar{p}_o\bar{h}_{\dot{y}}) - 2\Lambda\gamma(\bar{p}_{\dot{y}}\bar{h}_o + \bar{p}_o\bar{h}_{\dot{y}}) = 0 \tag{24}$$

Here, $\bar{p} = p/p_a$, $\bar{h} = h/c$, $\bar{w} = w/c$, $\phi = x/R$, $\bar{z} = z/R$, and $\bar{t} = \upsilon t$. And Λ and γ represent the bearing number (or compressibility number) and whirl frequency ratio, respectively. Those are as follows:

$$\Lambda = \frac{6\mu\omega}{p_a}\left(\frac{R}{c}\right)^2 \tag{25}$$

$$\gamma = \frac{\upsilon}{\omega} \tag{26}$$

The perturbed film thickness about each perturbation variables can be derived as follows:

$$\bar{h}_x = \frac{\bar{k}_e(\bar{p}_x - \bar{k}_e cos\theta) + \bar{c}_e\gamma(\bar{p}_{\dot{x}} - \bar{c}_e\gamma cos\theta)}{\bar{k}_e^2 + (\bar{c}_e\gamma)^2} \tag{27}$$

$$\bar{h}_{\dot{x}} = \frac{\bar{k}_e(\bar{p}_{\dot{x}} - \bar{k}_e cos\theta) + \bar{c}_e\gamma(\bar{p}_x - \bar{c}_e\gamma cos\theta)}{\bar{k}_e^2 + (\bar{c}_e\gamma)^2} \tag{28}$$

$$\bar{h}_y = \frac{\bar{k}_e(\bar{p}_y - \bar{k}_e sin\theta) + \bar{c}_e\gamma(\bar{p}_{\dot{y}} - \bar{c}_e\gamma sin\theta)}{\bar{k}_e^2 + (\bar{c}_e\gamma)^2} \tag{29}$$

$$\bar{h}_{\dot{y}} = \frac{\bar{k}_e(\bar{p}_{\dot{y}} - \bar{k}_e sin\theta) + \bar{c}_e\gamma(\bar{p}_{\dot{y}} - \bar{c}_e\gamma sin\theta)}{\bar{k}_e^2 + (\bar{c}_e\gamma)^2} \tag{30}$$

From above equations, it can be supposed that the bump stiffness, K_e, and damping, C_e, make the perturbed film thickness decreases and the perturbed pressure increases.

2.5. Static characteristics of the air foil bearings

The pressure distribution over the air film can be calculated using zeroth order equation (20). And finite difference method was adopted. The bearing area was divided into several grids with the uniform interval to the direction of x and y. Successive under relaxation (SUR) method which is good for safe convergence was applied. To compare the effect of the slip flow, the results with and without those terms were obtained respectively. After obtaining the pressure distribution, integrating it over the area, the hydrodynamic force can be

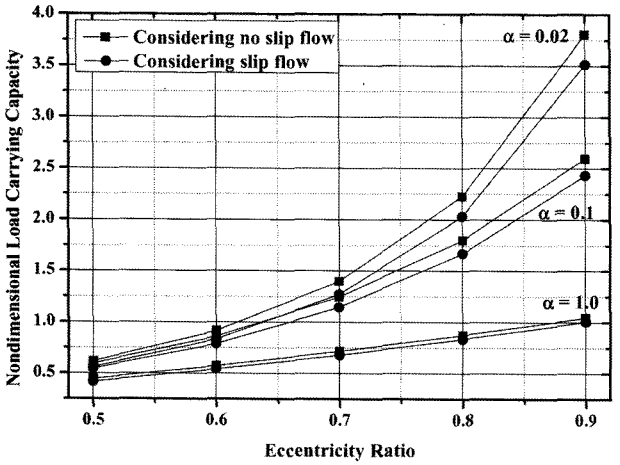

Fig. 5. Nondimensional load carrying capacity versus eccentricity ratio at $L/D = 1.0$, $\phi_0 = 0$ and $\Lambda = 1.0$.

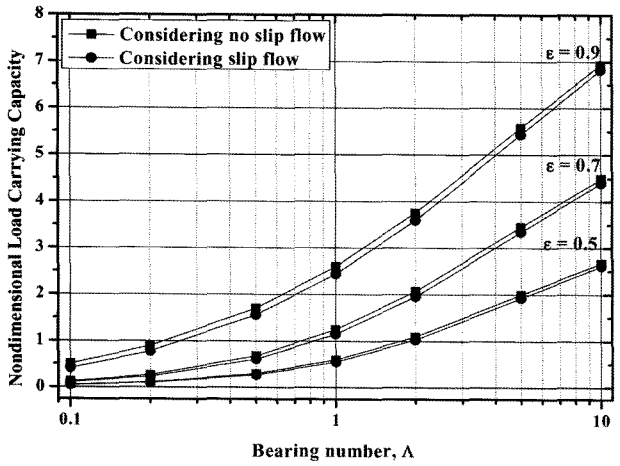

Fig. 6. Nondimensional load carrying capacity versus bearing number at $L/D = 1.0$, $\phi_0 = 0$ and $\alpha = 0.1$.

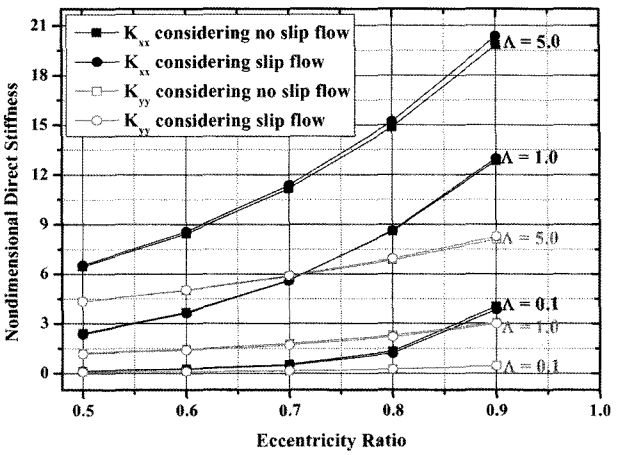

Fig. 7. Nondimensional direct stiffness versus eccentricity ratio at $L/D = 1.0$, $\phi_0 = 0$ and $\alpha = 0.1$.

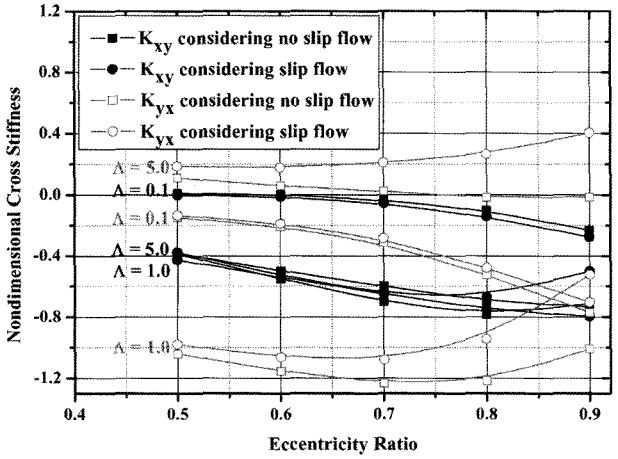

Fig. 8. Nondimensional cross stiffness versus eccentricity ratio at $L/D = 1.0$, $\phi_0 = 0$ and $\alpha = 0.1$.

calculated using following equation.

$$\begin{Bmatrix} \bar{F}_x \\ \bar{F}_y \end{Bmatrix} = \frac{1}{p_a R^2}\begin{Bmatrix} F_x \\ F_y \end{Bmatrix} = \int_{-1/2}^{1/2}\int_0^{2\pi}(\bar{p}-1)\begin{Bmatrix} cos\theta \\ sin\theta \end{Bmatrix} d\theta dz \quad (31)$$

The load carrying capacity and attitude at the equilibrium state are as follows:

$$\bar{W} = \frac{W}{p_a R^2} = \sqrt{\bar{F}_x^2 + \bar{F}_y^2} \quad (32)$$

$$\phi_0 = tan^{-1}\left(\frac{\bar{F}_y}{\bar{F}_x}\right) \quad (33)$$

2.6. Dynamic characteristics of the air foil bearings using perturbation method

To determine the dynamic characteristics of the air foil bearing, equation (21)-(24) were used with centraldifference method. The boundary conditions of the perturbed pressure are same as follows:

$$\left.\begin{aligned} \bar{p} &= 1 \\ \bar{p}_{\bar{x}} = \bar{p}_{\dot{\bar{x}}} &= \bar{p}_{\bar{y}} = \bar{p}_{\dot{\bar{y}}} = 0 \end{aligned}\right\} \quad \text{at} \quad \bar{z} = \pm 1/2 \quad (34)$$

$$\left.\begin{aligned} \bar{p} &= 1 \\ \bar{p}_{\bar{x}} = \bar{p}_{\dot{\bar{x}}} &= \bar{p}_{\bar{y}} = \bar{p}_{\dot{\bar{y}}} = 0 \end{aligned}\right\} \quad \text{at} \quad \theta = \theta_1,\ \theta_1 + 2\pi \quad (35)$$

The bearing stiffness and damping coefficients can be calculated by integrating the perturbed pressure over the bearing area. And those are as follows:

$$\begin{bmatrix} \bar{K}_{xx} & \bar{K}_{xy} \\ \bar{K}_{yx} & \bar{K}_{yy} \end{bmatrix} = \frac{c}{p_a R^2}\begin{bmatrix} K_{xx} & K_{xy} \\ K_{yx} & K_{yy} \end{bmatrix} = \int_{-L/D}^{L/D}\int_0^{2\pi}\begin{bmatrix} \bar{p}_{\bar{x}} cos\theta & \bar{p}_{\bar{y}} cos\theta \\ \bar{p}_{\bar{x}} sin\theta & \bar{p}_{\bar{y}} sin\theta \end{bmatrix} d\theta dz \quad (36)$$

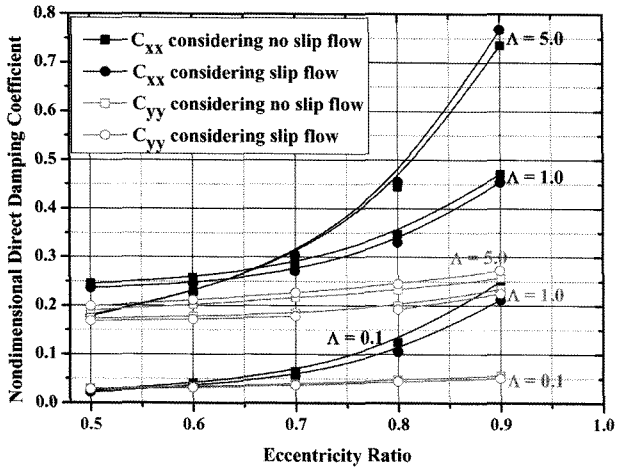

Fig. 9. Nondimensional direct damping coefficient versus eccentricity ratio at L/D = 1.0, ϕ_0= 0 and α = 0.1.

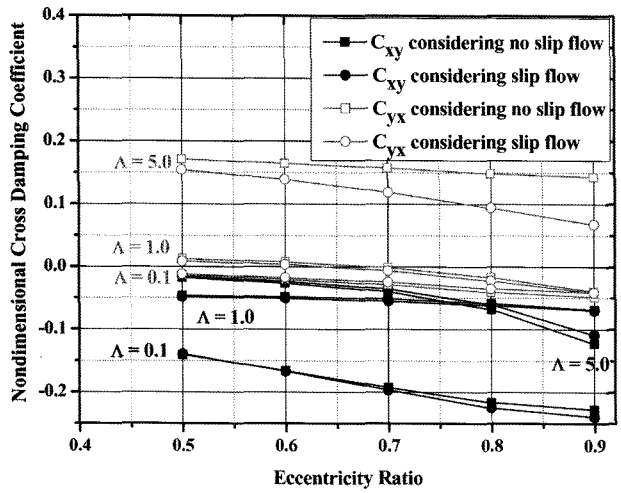

Fig. 10. Nondimensional cross damping coefficient versus eccentricity ratio at L/D = 1.0, ϕ_0= 0 and α = 0.1.

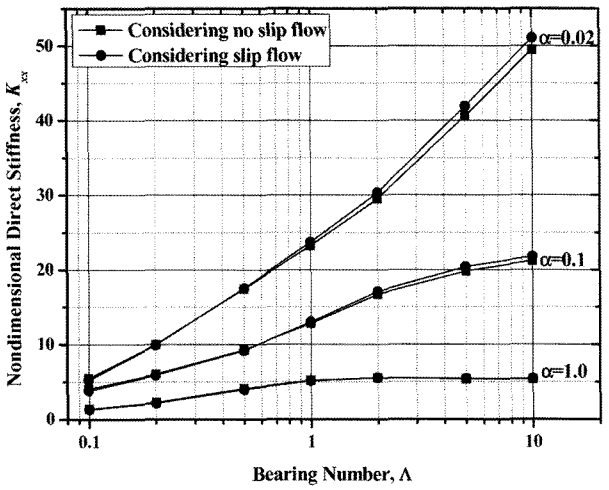

(a) Nondimensional direct stiffness, K_{xx}.

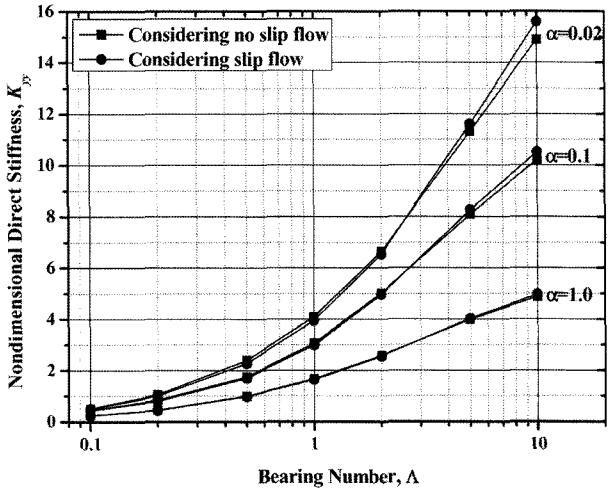

(b) Nondimensional direct stiffness, K_{yy}.

Fig. 11. Nondimensional direct stiffness versus bearing number at L/D = 1.0, ϕ_0=0 and ε = 0.9.

$$\begin{bmatrix} \bar{C}_{xx} & \bar{C}_{xy} \\ \bar{C}_{yx} & \bar{C}_{yy} \end{bmatrix} = \frac{c\omega}{p_a R^2}\begin{bmatrix} C_{xx} & C_{xy} \\ C_{yx} & C_{yy} \end{bmatrix} = \int_{-L/D}^{L/D}\int_0^{2\pi}\begin{bmatrix} \bar{p}_x\cos\theta & \bar{p}_y\cos\theta \\ \bar{p}_x\sin\theta & \bar{p}_y\sin\theta \end{bmatrix} d\theta d\bar{z} \tag{37}$$

3. Numercal Analysis Results

3.1. Static characteristics, load carrying capacity

Figure 5 and 6 present the nondimensional load carrying capacity versus eccentricity ratio and bearing number. Both the results considering no slip and slip flow were compared each other. Generally, the results with slip flow were more than those with no slip flow. And the difference between both cases increases as the bearing number increases and the eccentricity ratio increases. It can be explained using equation (19). At the condition of the constant bearing number, the pressure decreases relatively as the value of the rarefaction coefficient increases under slip flow regime.

3.2. Dynamic characteristics, stiffness and damping coefficients

In the case of the direct dynamic characteristics, the difference between the slip and no slip flow were little as shown to the Figure 7 and 9. And it increases as the bearing number and eccentricity increases as same as the static characteristics. Generally, xx elements were larger than the yy elements. It is because the journal is eccentric to the x direction. The cross dynamic characteristics were presented at Figure 8 and 10. Similarly with the results of the direct terms, the difference increases as the bearing number and eccentricity increases. And the difference magnitude was larger than those of the direct terms. Figure 11 to 14 show the dynamic characteristics under various bump compliance. The compliance is the reciprocal of the stiffness. And the results show that the direct terms increases as the bump stiffness increases. The difference

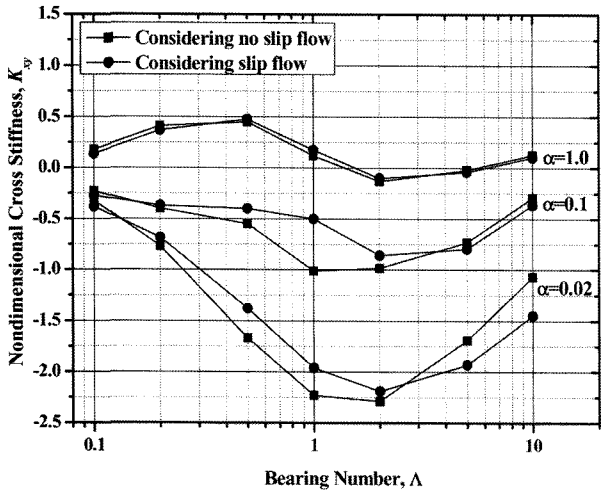

(a) Nondimensional cross stiffness, K_{xy}.

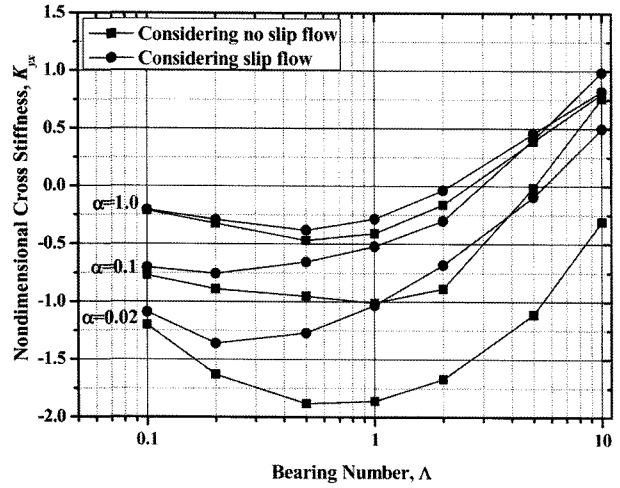

(b) Nondimensional cross stiffness, K_{yx}.

Fig. 12. Nondimensional cross damping coefficient versus eccentricity ratio at L/D = 1.0, ϕ_0 = 0 and ε = 0.9.

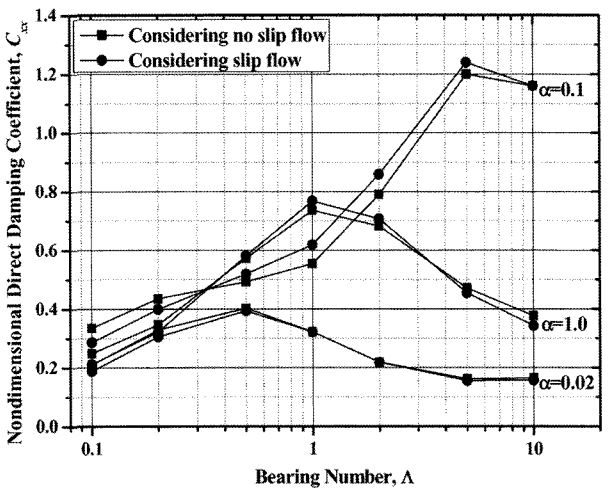

(a) Nondimensional direct damping, C_{xx}.

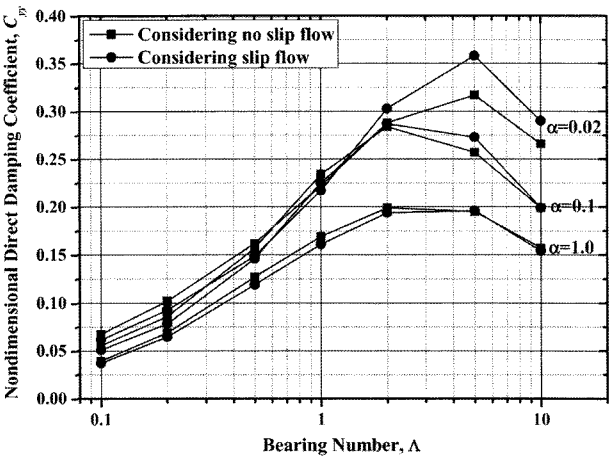

(b) Nondimensional direct damping, C_{yy}.

Fig. 13. Nondimensional direct damping coefficient versus eccentricity ratio at L/D = 1.0, ϕ_0 = 0 and ε = 0.9.

between the results of two flow models was little as much to be able to ignore. But in the case of the cross terms, the difference is larger at small compliance. The cross terms plays an important role to determine the rotor dynamic stability of the rotating journal and in the rotor dynamic analysis, proposed slip flow model can be taken into consideration for more reliable analysis.

4. Conclusion

In this paper, the slip flow effect to the air foil journal bearing analysis was investigated. And the results can be summarized as follows:

(1) The load carrying capacity increases as the eccentricity ratio and bearing number increase and the bump compliance decreases.

(2) The maximum difference between the results considering slip flow and no slip flow is about 10% and the difference increases as the load carrying capacity increases.

(3) In the case of the direct dynamic characteristics, the difference between the slip and no slip flow were little as much to be able to ignore and it increases as the bearing number and eccentricity increases as same as the static characteristics.

(4) But in the case of the cross terms of the dynamic characteristics, the difference is larger at small compliance.

The results from this analysis can be used for more reliable rotor dynamic analysis.

Acknowledgments

This work was supported by a grant from "Development of intelligent sensors & actuators for high speed rotating machinery" project of the Korea Institute of Science and Technology, "Standardization of test method for Air Foil Bearing and Turbo Blower" project of Ministry of Commerce, Industry and Energy, and "The development of a high-speed motor system" project of Korea Energy Management Corporation, Korea. The authors thank to KIST, MOCIE and KEMCO.

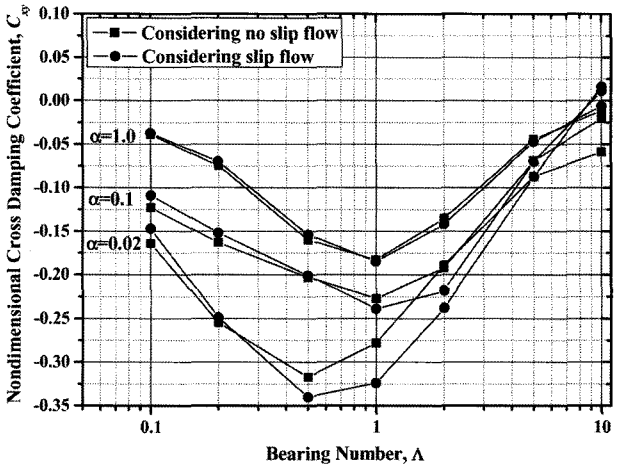

(a) Nondimensional cross damping, C_{xy}.

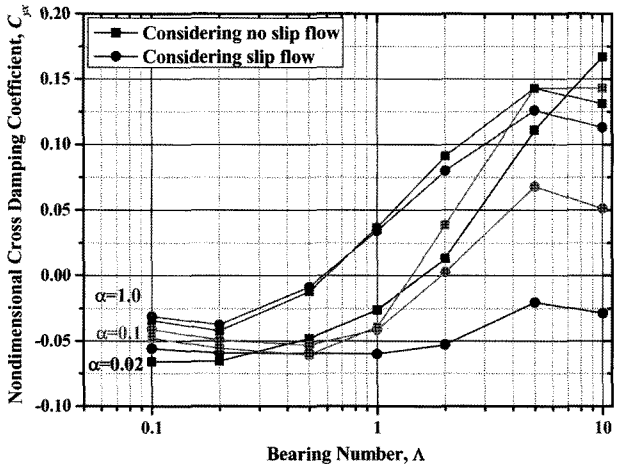

(b) Nondimensional cross damping, C_{yx}.

Fig. 14. Nondimensional cross damping coefficient versus eccentricity ratio at L/D=1.0, ϕ_0= 0 and ε= 0.9.

References

1. Block, H., and Van Ressum, J. J., "The Foil Bearing-A New Departure in Hydrodynamic Lubrication," Lubrication Engineering, Vol. 9, No. 6, pp. 316-320, 1953.
2. Arakere, N. K. and Nelson, H. D., "An Analysis of Gas-Lubricated Foil Journal Bearings," Tribology Transactions, Vol. 35, No. 1, pp. 1-10, 1992.
3. Walowit, J. A. and Anno, J. N., "Modern Development in Lubrication Mechanics," Applied Science Publishers, London, 1975.
4. Lund, J. W., "Calculation of Stiffness and Damping Properties of Gas Bearings," ASME Journal of Lubrication Technology, 90, pp 793-803, 1968.
5. DellaCorte, C., Zaldana, A. R., and Radil, K., C., "A System Approach to the Solid Lubrication Foil Air Bearings for Oil-Free Turbomachinery," NASA/TM-2002-211482, 2002.
6. DellaCorte, C., Lukaszewicz, V., Valco, M. J., Radil, K. C., and Heshmat, H., "Performance and Duarability of High Temperature Foil Air Bearings for Oil-Free Turbomachin-ery, "Tribology Transactions, Vol. 43, No. 4, pp. 774-780, 2000.
7. Lee, N. S., Choi, D. H., Lee, Y. B., Kim, T. H., and Kim, C. H., 2002, "The Influence of the Slip Flow on Steady-State Load Capacity, Stiffness and Damping Coefficients of Elastically Supported Gas Foil Bearings," Tribology Transaction, 45, pp. 478-484.
8. EL Hak, M. G., "The Fluid Mechanics of Microdevices-the Freeman Scholar Lecture," Journal of Fluids Engineering," Vol. 121, pp. 5-33, 1999.
9. Park, D. J., Kim, C. H., and Lee, Y. B., "Static and Dynamic Characteristics of Air Foil Thrust Bearing Considering Tilting Pad Condition," GT 2007-27814, 2007.
10. Heshmat, H., Walowit, J.A. and Pinkus, O., "Analysis of Gas-Lubricated Foil Journal Bearings," Journal of Lubrication Technology, 105. pp. 647-655, 1983.
11. Ruscitto, D., Mc Cormick, J., and Gray, S., "Hydrodynamic Air Lubricated Compliant Surface Bearing For An Automotive Gas Turbine Engine I - Journal Bearing Performance," NASA CR-135368, 1978.